

# Broad Band Optical Polarimetric Study of IC 1805

Biman J. Medhi<sup>1</sup>\*, Maheswar G.<sup>1</sup>, Brijesh K.<sup>1</sup>, J.C. Pandey<sup>2</sup>, T.S. Kumar<sup>1</sup>, Ram Sagar<sup>1</sup>

<sup>1</sup>*Aryabhata Research Institute of Observational Sciences, Manora Peak, Nainital - 263 129, India*

<sup>2</sup>*Tata Institute of Fundamental Research, Homi Bhabha Road, Mumbai - 400 005, India*

## ABSTRACT

We present the *BVR* broad band polarimetric observations of 51 stars belonging to the young open cluster IC 1805. Along with the photometric data from the literature we have modeled and subtracted the foreground dust contribution from the maximum polarization ( $P_{max}$ ) and colour excess ( $E_{B-V}$ ). The mean value of the  $P_{max}$  for *intraccluster* medium and the foreground are found to be  $5.008 \pm 0.005\%$  and  $4.865 \pm 0.022\%$  respectively. Moreover, the mean value of the wavelength of maximum polarization ( $\lambda_{max}$ ) for *intraccluster* medium is  $0.541 \pm 0.003 \mu m$ , which is quite similar as the general interstellar medium (ISM). The resulting *intraccluster* dust component is found to have negligible polarization efficiency as compared to interstellar dust. Some of the observed stars in IC 1805 have shown the indication of intrinsic polarization in their measurements.

**Key words:** ISM: dust, extinction, polarization - open clusters: individual (IC 1805)

## 1 INTRODUCTION

Polarization of starlight is one among a number of properties manifested by interstellar dust grains. Wavelength dependence of polarization, for instance, can give information on the size distribution of grains towards different Galactic directions. Polarization is thought to be caused by the same dust grain responsible for the reddening of starlight. According to Davis and Greenstein mechanism (Davis *et al.*, 1951), the polarization of starlight is caused by the selective extinction due to the elongated dust grains aligned in space possibly due to magnetic field.

In order to investigate the distribution and characteristic of dust grains, we have selected the young open cluster IC 1805. The reddening law is anomalous in this direction and the extinction is non uniform over the cluster region (Sagar 1987; Borgman 1961; Johnson 1968; Ishida 1969; Turner 1976). The polarimetric components produced by the Galactic dust located in front of the cluster can be found out from maximum polarization  $P_{max}$  and colour excess  $E_{B-V}$  (Marraco *et al.* 1993). By removing the effect of dust located on the line of sight from the data, one can study the component associated with the internal extinction of the cluster. The young and rich open cluster IC 1805 (*R.A.*(J2000) :  $02^h 32^m 42^s$ , *Dec* (J2000) :  $+61^d 27^m 00^s$ ) is the core of the CasOB6 association. It is located in the Perseus spiral arm, radially outward from the local spiral arm. IC 1805 is situated in a HII region and embedded in W4

molecular cloud. The colour excess  $E_{(B-V)}$  for the cluster members varies from 0.52 to 1.3 mag (Joshi & Sagar 1983). From the near-IR study of IC 1805, Sagar *et al.* (1990) found that the distribution of dust and patchy ionized gas appear to be the cause of non uniform extinction across the cluster face. The relative proper-motion cluster membership study was done by Vasilevskis *et al.* (1965) in a field of about 0.66 square degree, centered on the O type giant VSA 148 for 350 stars with a mean error of  $\pm 0.16''/\text{century}$ . Sanders (1972) revised these membership probabilities by applying the maximum-likelihood method. The recent estimation of cluster distance is  $\simeq 2.4$  kpc (Joshi & Sagar 1983), though the earlier estimate varies from 1.6 to 2.5 kpc.

The previous polarimetric study on IC 1805 was carried out by Guetter *et al.* (1989), for 24 member stars brighter than visual magnitude of  $\simeq 12$  mag. In order to study details about the grain alignment and particle size distribution we have observed 32 member stars (nine star common with Guetter *et al.* 1989) brighter than visual magnitude of  $\simeq 15.5$  mag in IC 1805. The next section describes the details of instrumentation, observation and data reduction while the main results are given and discussed in the remaining part of the paper.

## 2 INSTRUMENTATION AND OBSERVATION

The ARIES Imaging Polarimeter (AIMPOL) consists of a half wave plate (HWP) modulator and a beam-splitting Wollaston prism analyzer placed in the telescope beam path to

\* E-mail: biman@aries.ernet.in

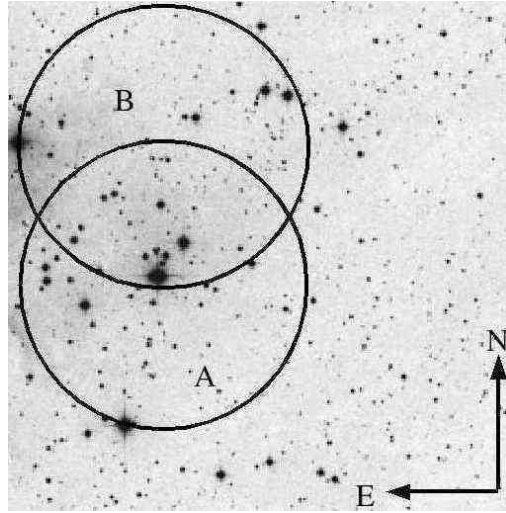


**Figure 1.** The  $11.00' \times 11.00'$  B-band image of the fields A & B of IC 1805, reproduced from Digitized Sky Survey.

**Table 1.** Observed polarized standard stars

Star name	Filter	$P \pm \epsilon_P$ (%)	$\theta \pm \epsilon_\theta$ ( $^\circ$ )	$P \pm \epsilon_P$ (%)	$\theta \pm \epsilon_\theta$ ( $^\circ$ )
Published data					
Hiltner-960	B	$5.72 \pm 0.06$	$55.06 \pm 0.31$	$5.60 \pm 0.21$	$54.62 \pm 1.08$
	V	$5.66 \pm 0.02$	$54.79 \pm 0.11$	$5.71 \pm 0.15$	$53.32 \pm 0.05$
	R	$5.21 \pm 0.03$	$54.54 \pm 0.16$	$5.19 \pm 0.06$	$54.81 \pm 0.34$
HD204827	B	$5.65 \pm 0.02$	$58.20 \pm 0.11$	$5.75 \pm 0.09$	$58.63 \pm 0.45$
	V	$5.32 \pm 0.02$	$58.73 \pm 0.08$	$5.36 \pm 0.03$	$60.19 \pm 0.17$
	R	$4.89 \pm 0.03$	$59.10 \pm 0.17$	$4.90 \pm 0.23$	$58.82 \pm 1.14$
BD+64°106	B	$5.51 \pm 0.09$	$97.15 \pm 0.47$	$5.44 \pm 0.10$	$99.42 \pm 0.51$
	V	$5.69 \pm 0.04$	$96.63 \pm 0.18$	$5.49 \pm 0.13$	$97.06 \pm 0.17$
	R	$5.15 \pm 0.10$	$96.74 \pm 0.54$	$5.21 \pm 0.02$	$97.38 \pm 0.11$
HD19820	B	$4.70 \pm 0.04$	$115.70 \pm 0.22$	$4.84 \pm 0.23$	$113.42 \pm 0.11$
	V	$4.79 \pm 0.03$	$114.93 \pm 0.17$	$4.92 \pm 0.11$	$114.50 \pm 0.11$
	R	$4.53 \pm 0.03$	$114.46 \pm 0.17$	$4.73 \pm 0.14$	$113.82 \pm 0.28$

produce ordinary and extraordinary images in slightly different directions separated by about 27 pixel.

A focal reducer (85mm, f/1.8) is placed between Wollaston prism and CCD camera. The detail descriptions about the AIMPOL are available in Rautela *et al.* (2004) (also see Ramaprakash *et al.* 1998).

By definition, the ratio  $R(\alpha)$  is given by,

$$R(\alpha) = \frac{I_o/I_e - 1}{I_o/I_e + 1} = P \cos(2\theta - 4\alpha) \quad (1)$$

which is the difference between the intensities of the ordinary ( $I_o$ ) and extraordinary ( $I_e$ ) beams to their sum,  $P$  is the fraction of the total light in the linearly polarized condition and  $\theta$  is the position angle of plane of polarization. It is denoted by normalized Stokes' parameter  $q$  ( $= Q/I$ ), when the half wave plate's fast axis is aligned to the reference axis ( $\alpha = 0^\circ$ ). Similarly, the normalized Stokes' parameter  $u$  ( $= U/I$ ),  $q_1$  ( $= Q_1/I$ ),  $u_1$  ( $= U_1/I$ ) are also the ratios  $R(\alpha)$ , when the half wave plate are at  $22.5^\circ$ ,  $45^\circ$  and  $67.5^\circ$  respectively. In principle,  $P$  and  $\theta$  can be determined by using only two Stokes' parameters  $q$  and  $u$ . In reality, the situation is not so simple because of two reasons (i) the

responsivity of the system to the two orthogonal polarization components may not be same and (ii) the responsivity of the CCD is a function of position on its surface. So, the signals which are actually measured in the two images ( $I'_o$  and  $I'_e$ ) may differ from the observed one by the following formula (Ramaprakash 1998)

$$\frac{I'_o(\alpha)}{I'_e(\alpha)} = \frac{I_o(\alpha)}{I_e(\alpha)} \times \frac{F_o}{F_e} \quad (2)$$

and the Eq.(1) can be rewrite as

$$R(\alpha) = \frac{(I_o/I_e \times F_o/F_e) - 1}{(I_o/I_e \times F_o/F_e) + 1} = P \cos(2\theta - 4\alpha) \quad (3)$$

where  $F_o$  and  $F_e$  represent the effects mentioned above and the ratio is given by,

$$\frac{F_o}{F_e} = \left[ \frac{I'_o(0^\circ)}{I'_e(45^\circ)} \times \frac{I'_o(45^\circ)}{I'_e(0^\circ)} \times \frac{I'_o(22.5^\circ)}{I'_e(67.5^\circ)} \times \frac{I'_o(67.5^\circ)}{I'_e(22.5^\circ)} \right]^{1/4} \quad (4)$$

Substituted the ratio in Eq.(3) and fitting the cosine curve to the four values of  $R(\alpha)$ , the values of  $P$  and  $\theta$  could be obtained. The individual errors associated with the four val-

**Table 2.** Observed *BVR* polarization values for different stars in IC 1805

Id	<i>M<sub>V</sub></i> (mag)	<i>P<sub>B</sub></i> ± $\epsilon_p$ (%)	$\theta_B$ ± $\epsilon_\theta$ (°)	<i>P<sub>V</sub></i> ± $\epsilon_p$ (%)	$\theta_V$ ± $\epsilon_\theta$ (°)	<i>P<sub>R</sub></i> ± $\epsilon_p$ (%)	$\theta_R$ ± $\epsilon_\theta$ (°)
112 <sup>G</sup>	09.91	6.42±0.09	121.3±0.4	6.80±0.09	121.1±0.1	6.40±0.14	120.7±0.6
118 <sup>G</sup>	10.30	5.89±0.15	122.8±0.2	5.90±0.01	121.5±0.1	5.79±0.01	121.3±0.6
121	11.59	6.20±0.18	126.8±0.7	6.35±0.09	126.7±0.3	5.96±0.09	126.4±0.4
122	13.73	4.99±0.61	120.6±3.6	5.10±0.51	118.5±0.1	5.04±0.43	118.6±2.4
123	13.88	2.90±0.14	121.6±1.4	3.84±0.18	120.2±1.3	3.05±0.15	121.6±0.3
128	13.40	3.41±0.12	108.7±0.8	3.92±0.17	120.0±1.0	3.80±0.09	118.8±0.6
129	14.06	5.07±0.18	123.4±1.3	5.78±0.14	126.2±1.2	5.21±0.18	124.5±1.4
130*	13.26	4.75±0.30	124.0±0.5	5.53±0.03	124.5±1.0	5.15±0.04	126.5±0.1
133*	13.56	3.28±0.38	118.3±3.3	3.64±0.19	125.9±1.5	3.30±0.48	123.4±4.1
136 <sup>G</sup>	11.04	5.39±0.10	121.9±0.5	5.41±0.09	119.9±0.4	5.38±0.04	120.9±0.2
138 <sup>G</sup>	09.58	5.80±0.08	122.9±0.4	6.31±0.08	119.0±0.3	5.40±0.36	120.0±2.3
139	13.10	5.12±0.04	123.1±0.2	5.30±0.17	119.3±0.8	5.10±0.07	121.0±0.4
143	11.40	4.68±0.04	125.4±0.2	5.25±0.05	122.5±0.2	4.80±0.07	122.6±0.4
146*	13.53	5.44±0.56	124.7±2.9	5.72±0.34	117.3±1.7	4.97±0.07	119.4±0.4
147	13.34	4.23±0.30	122.6±3.2	4.86±0.15	122.1±0.8	4.71±0.17	122.2±0.9
149 <sup>G</sup>	11.24	4.37±0.09	122.4±0.5	4.93±0.09	119.6±0.5	4.56±0.05	118.3±0.3
154	14.07	4.19±0.59	114.7±3.8	4.27±0.23	115.6±1.5	4.07±0.25	123.8±1.8
155*	14.39	4.95±0.66	111.5±3.8	4.52±0.17	116.6±1.0	4.35±0.09	111.3±0.6
156 <sup>G</sup>	12.03	4.19±0.05	122.2±0.3	4.28±0.04	120.6±0.2	3.55±0.17	122.6±1.3
157	13.48	5.17±0.29	121.4±1.2	5.67±0.30	119.8±1.5	5.54±0.05	120.8±0.2
158	12.73	3.98±0.11	122.9±4.4	4.50±0.10	126.1±0.6	4.27±0.02	127.5±0.1
160 <sup>G</sup>	08.11	5.58±0.19	117.4±0.9	5.91±0.46	117.5±2.2	5.30±0.06	117.4±0.3
162	12.55	5.63±0.46	121.9±2.3	5.77±0.08	118.3±0.4	5.57±0.22	119.5±1.2
165	12.77	5.23±0.14	122.4±0.7	5.68±0.16	119.0±0.8	5.18±0.04	119.3±0.2
166	11.97	4.74±0.31	119.6±1.3	4.99±0.29	119.2±0.2	4.49±0.14	120.5±0.2
168	13.72	6.06±0.82	122.0±0.8	5.29±0.34	117.1±1.8	5.16±0.10	119.3±0.5
170	10.07	3.52±0.09	121.2±0.1	3.75±0.07	118.3±0.5	3.44±0.26	118.8±2.1
171	13.13	5.16±0.13	124.0±0.6	5.24±0.14	115.4±2.0	5.13±0.05	119.5±0.3
173*	13.81	2.67±0.12	112.3±1.2	2.62±0.09	116.0±1.0	2.59±0.09	118.8±0.1
174	11.63	5.29±0.17	119.5±0.8	5.27±0.01	118.3±0.1	5.06±0.02	117.9±0.1
175	13.10	4.68±0.44	114.4±2.5	4.96±0.24	115.1±1.3	4.48±0.14	116.1±0.8
182	13.38	5.61±0.05	117.0±0.1	5.94±0.09	122.9±1.0	5.53±0.02	121.1±0.2
183 <sup>G</sup>	11.15	5.19±0.37	121.0±2.0	5.01±0.04	118.5±0.2	4.89±0.06	118.5±0.3
184*	13.64	4.20±0.28	120.4±1.6	3.82±0.11	120.0±0.7	3.81±0.16	124.6±1.2
185*	11.58	5.56±0.05	121.9±0.2	5.44±0.19	120.1±0.9	4.99±0.07	120.2±0.3
188	12.68	4.90±0.12	122.8±0.8	5.38±0.09	121.2±0.4	4.76±0.18	118.1±0.4
191	12.96	3.99±0.11	113.0±1.0	4.32±0.18	105.8±6.4	3.97±0.09	117.5±0.7
192 <sup>G</sup>	08.43	3.38±0.16	123.0±1.0	3.52±0.11	115.0±0.8	3.31±0.18	118.4±1.6
354*	13.43	4.75±0.35	125.9±1.7	4.82±0.31	116.7±6.7	4.28±0.05	119.2±0.3
359*	14.55	2.82±0.89	103.8±9.0	4.10±0.30	117.4±1.6	3.76±0.15	122.6±1.1
360*	14.52	3.14±0.41	121.3±3.6	3.10±0.09	123.2±0.8	3.31±0.45	123.2±3.8
362*	14.48	4.66±0.25	121.4±2.8	5.46±0.27	119.7±0.9	4.70±0.02	117.2±0.1
363*	14.61	4.77±0.41	101.8±14.8	5.77±0.27	118.0±1.3	4.60±0.30	119.7±2.1
365*	14.56	4.41±0.21	120.8±1.3	4.33±0.04	116.2±0.2	3.88±0.64	120.8±6.3
424*	14.41	4.61±0.68	122.7±4.3	4.57±0.02	124.9±0.1	4.46±0.02	116.4±0.1
426*	15.11	6.12±1.02	121.8±4.1	5.36±0.22	119.7±1.1	5.12±0.12	120.8±1.1
429*	14.92	5.19±0.94	120.8±5.2	4.82±0.14	113.6±1.0	4.96±0.16	121.4±2.5
470*	14.03	5.12±0.31	117.4±1.7	4.69±0.05	115.1±0.3	4.20±0.02	118.4±0.1
480*	15.47	7.84±1.52	116.9±8.9	6.56±0.93	123.0±4.0	6.78±0.45	120.7±1.9
541*	13.71	4.96±0.70	120.7±5.0	5.54±0.46	119.7±2.3	5.18±0.86	120.6±4.7
552*	14.47	7.39±0.05	110.1±0.2	7.28±0.13	113.6±4.4	6.86±0.58	118.9±2.4

\* : Nonmember

<sup>G</sup> : Common with Guetter *et al.* 1989

ues of  $R(\alpha)$  putting as a weight while calculating  $P$ ,  $\theta$  and their respective errors.

The optical imaging polarimetry of the two fields A and B (see Figure 1) in IC 1805 was carried out to study the contribution of interstellar and *intracluster* material on linear polarization. The data were obtained on 12<sup>th</sup> and 13<sup>th</sup> October, 2006 using the TK 1024 × 1024 pixel<sup>2</sup> CCD cam-

era mounted on the Cassegrain focus of the 104-cm Sampurnanand telescope of ARIES, Nainital in *B*, *V* and *R* ( $\lambda_{B_{eff}}=0.440\text{ }\mu\text{m}$ ,  $\lambda_{V_{eff}}=0.550\text{ }\mu\text{m}$  and  $\lambda_{R_{eff}}=0.660\text{ }\mu\text{m}$ ) photometric bands. Each pixel of the CCD corresponds to 1.73 arcsec and the field of view is ∼ 8 arcmin diameter on the sky. The FWHM of the stellar image varies from 2 pixel to 3 pixel. The read out noise and gain of the CCD are 7.0

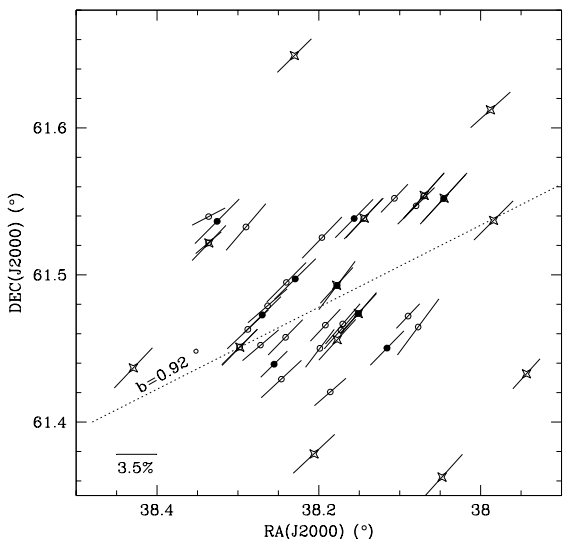


**Figure 2.** Polarization vectors and their orientations for the stars of IC 1805. The vectors are proportional to the magnitude of the polarization. The scale is indicated in the figure. Filled and open circles indicate members and nonmembers of cluster IC 1805 observed by us and the starmark indicate the stars observed by Guetter *et al.* (1989). The dotted line is the galactic parallel  $b = 0.92^\circ$

$e^-$  and  $11.98 e^-/\text{ADU}$  respectively. The fluxes for all of our programme stars were extracted by aperture photometry after the bias subtraction in the standard manner using IRAF. Instead of robust flat fielding technique we are using Eq.[3] to make uniform response, as mentioned above.

Standard stars for null polarization and for the zero point of the polarization position angle were taken from Schmidt *et al.* (1992). The results for polarized standards are given in Table 1. From the results we can conclude that the observed polarization and position angles are matching with Schmidt *et al.* (1992) within the error limit. The average value of instrumental polarization is found to be about  $\sim 0.04\%$ .

The AIMPOL does not have a grid placed to avoid the overlapping of ordinary image with the extraordinary image of an adjacent region 27 pixels away from it. In the care of target sources, we have selected (usually) only those which are well isolated. But, due to the overlapping, sky at a region gets doubled. However, we found the sky variation at different location to be not very significant. Therefore, the effect gets canceled when we consider both ordinary and extraordinary images of these target sources for the analysis.

### 3 RESULTS

Table 2 lists, for the 51 observed stars in the direction of IC 1805, the percentage of polarization, the position angle of the plane of polarization in the equatorial coordinate system and their respective errors for each filters. Membership probabilities, star identification numbers (Id) for all observed stars are taken from Sanders (1972) and the visual

**Table 3.** Polarization results for IC 1805 stars

Id	$P_{max} \pm \epsilon$ (%)	$\sigma_1$	$\lambda_{max} \pm \epsilon$ ( $\mu m$ )	$E_{B-V}$
112 <sup>†</sup>	$6.76 \pm 0.04$	0.66	$0.54 \pm 0.01$	0.82
118	$5.92 \pm 0.02$	2.96	$0.57 \pm 0.01$	0.85
121	$6.38 \pm 0.01$	0.05	$0.52 \pm 0.01$	0.88
122	$5.20 \pm 0.08$	0.25	$0.55 \pm 0.02$	—
123	$3.32 \pm 0.33$	3.40	$0.58 \pm 0.13$	0.79
128	$3.85 \pm 0.05$	0.68	$0.60 \pm 0.02$	0.97
129 <sup>†</sup>	$5.58 \pm 0.20$	2.00	$0.56 \pm 0.06$	0.81
130*	$5.54 \pm 0.09$	2.21	$0.51 \pm 0.02$	—
133*	$3.59 \pm 0.08$	0.50	$0.56 \pm 0.05$	—
136	$5.58 \pm 0.10$	2.23	$0.55 \pm 0.02$	0.89
138 <sup>†</sup>	$6.26 \pm 0.18$	2.06	$0.56 \pm 0.04$	0.79
139 <sup>†</sup>	$5.35 \pm 0.01$	0.31	$0.54 \pm 0.01$	0.76
143	$5.10 \pm 0.15$	4.15	$0.57 \pm 0.04$	0.86
146*	$5.69 \pm 0.27$	0.70	$0.47 \pm 0.03$	—
147	$4.82 \pm 0.07$	0.68	$0.59 \pm 0.03$	0.78
149 <sup>†</sup>	$4.75 \pm 0.10$	2.33	$0.56 \pm 0.03$	0.70
154	$4.30 \pm 0.03$	0.13	$0.53 \pm 0.01$	0.96
155*	$4.60 \pm 0.16$	0.90	$0.53 \pm 0.04$	—
156	$4.29 \pm 0.08$	2.41	$0.50 \pm 0.03$	0.88
157	$5.65 \pm 0.01$	0.13	$0.58 \pm 0.01$	0.89
158	$4.38 \pm 0.06$	1.45	$0.57 \pm 0.02$	1.24
160	$5.73 \pm 0.06$	0.48	$0.51 \pm 0.01$	1.02
162 <sup>†</sup>	$5.78 \pm 0.13$	0.36	$0.54 \pm 0.02$	0.67
165	$5.50 \pm 0.10$	1.31	$0.53 \pm 0.02$	0.86
166	$4.90 \pm 0.09$	0.51	$0.50 \pm 0.02$	0.75
168	$5.57 \pm 0.37$	1.04	$0.51 \pm 0.06$	0.96
170 <sup>†</sup>	$3.73 \pm 0.04$	0.63	$0.55 \pm 0.01$	0.35
171	$5.36 \pm 0.07$	0.96	$0.54 \pm 0.01$	0.76
173*	$2.70 \pm 0.06$	1.11	$0.53 \pm 0.04$	—
174 <sup>†</sup>	$5.27 \pm 0.03$	1.73	$0.54 \pm 0.01$	0.75
175	$4.92 \pm 0.12$	0.53	$0.50 \pm 0.02$	0.85
182	$5.85 \pm 0.03$	1.15	$0.53 \pm 0.01$	0.81
183	$5.02 \pm 0.05$	1.40	$0.56 \pm 0.03$	0.88
184*	$3.96 \pm 0.22$	1.82	$0.51 \pm 0.08$	—
185*	$5.61 \pm 0.01$	0.25	$0.48 \pm 0.01$	—
188 <sup>†</sup>	$5.26 \pm 0.15$	2.19	$0.54 \pm 0.05$	0.78
191	$4.19 \pm 0.05$	0.77	$0.54 \pm 0.02$	0.88
192	$3.52 \pm 0.01$	0.11	$0.53 \pm 0.01$	0.76
354*	$4.84 \pm 0.09$	0.34	$0.48 \pm 0.01$	—
359*	$3.90 \pm 0.26$	1.15	$0.56 \pm 0.11$	—
360*	$3.12 \pm 0.08$	0.86	$0.55 \pm 0.10$	—
362*	$5.01 \pm 0.26$	1.88	$0.52 \pm 0.05$	—
363*	$5.36 \pm 0.53$	2.33	$0.50 \pm 0.12$	—
365*	$4.44 \pm 0.01$	0.06	$0.47 \pm 0.01$	—
424*	$4.58 \pm 0.01$	0.54	$0.57 \pm 0.01$	—
426*	$5.47 \pm 0.24$	0.89	$0.52 \pm 0.05$	—
429*	$4.95 \pm 0.12$	1.01	$0.62 \pm 0.06$	—
470*	$4.88 \pm 0.08$	0.85	$0.46 \pm 0.01$	—
480*	$7.24 \pm 0.70$	0.87	$0.51 \pm 0.09$	—
541*	$5.46 \pm 0.11$	0.29	$0.57 \pm 0.04$	—
552*	$7.45 \pm 0.02$	0.41	$0.48 \pm 0.01$	—

\* : Nonmember

† : Frontside stars

magnitude  $M_V$  taken from the work of Joshi & Sagar (1983) and Massey *et al.* (1995). The stars with membership probability greater than 50% are considered as the members of IC 1805. Our results for the common stars are in agreement with Guetter *et al.* (1989) within the error limit except  $P_B$ . There is a systematic increments of  $\sim 0.45\%$  in  $P_B$  measurements for our values from those of Guetter *et al.* (1989).

The polarization map for all the stars of IC 1805 ob-

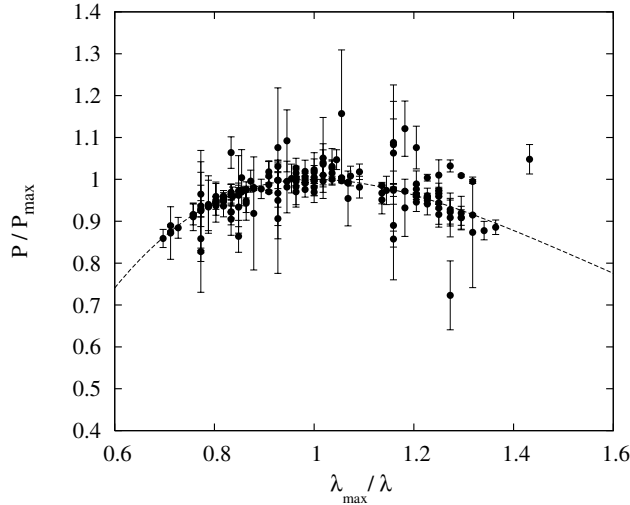


**Figure 3.** Plot of normalized polarization-wavelength dependence for the observed stars in IC 1805 determined from data listed in Tables 2 and 3. The error bars represent the uncertainties for the measurements of  $P/P_{max}$  and the solid curve denotes the Serkowski polarization relation for general interstellar medium (ISM) [Eq. (5)].

served by us and Guetter *et al.* (1989) is shown in Figure 2. The length of the polarization vectors are proportional to the degree of polarization ( $P_V$ ) in % (scale is given in the polarization map). The polarization vectors make an angle ( $\theta_V$ ) with the North-South axis (reference axis), which is given in column 6 of Table 2. The filled and open circles indicate the cluster member and nonmember of IC 1805 observed by us and the starmark indicate the stars observed by Guetter *et al.* (1989). From the polarization map we can conclude that the alignment of the polarization vectors over the whole observed area are close to being parallel to each other and there is no significant difference between the alignment of the star observed by us and Guetter *et al.* (1989). The alignment of member and nonmember stars of cluster IC 1805 are also closely parallel to each other. The orientation of the polarization vectors for the observed stars of IC 1805 indicate that the magnetic field in the direction of the cluster follow a general trend of the polarization directions in the region. The polarization in the cluster has an average direction of  $\bar{\theta}_V = 119.96 \pm 0.05$  in equatorial coordinate system. The dotted line superimposed on the Figure 2 is the galactic parallel  $b = 0.92^\circ$  showing a close alignment of the polarization vectors with the projection of the Galactic plane.

#### 4 DUST PROPERTIES

The wavelength ( $\lambda_{max}$ ) at which maximum polarization ( $P_{max}$ ) occurs is a function of the optical properties and characteristic of particle size distribution of the aligned dust grains (Wilking *et al.* 1980; McMillan 1978). Moreover, it is also related to the interstellar extinction law (Serkowski *et al.* 1975; Whittet *et al.* 1978; Coyne *et al.* 1979; Clayton *et*

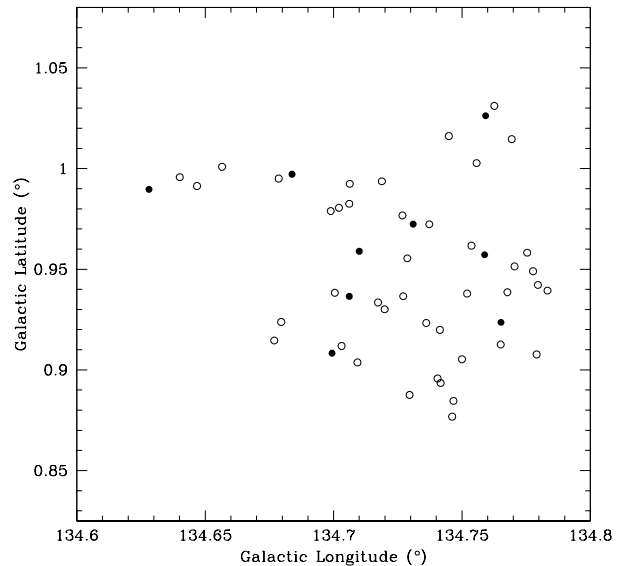


**Figure 4.** Galactic distribution for all observed stars of IC 1805. Filled circles indicate the *frontside* stars.

*al.* 1988). The maximum wavelength  $\lambda_{max}$  and polarization  $P_{max}$  have been calculated by fitting the observed polarization in the *BVR* band-passes to the standard Serkowski's polarization law,

$$P_\lambda / P_{max} = \exp [-k \ln^2 (\lambda_{max}/\lambda)] \quad (5)$$

and adopting the parameter  $k = 1.15$  (Serkowski 1973). If the polarization is well represented by the Serkowski relation,  $\sigma_1$  (the unit weight error of the fit) should not be higher than 1.6 due to the weighting scheme; a higher value could be indicative of the presence of intrinsic polarization. In fitting the degree of freedom is adopted as one. Though there are only three data points, the wavelength convey ranges from 0.44 to 0.66  $\mu\text{m}$  and all the  $\lambda_{max}$  found to fall within this range.

Table 3 represent  $P_{max}$ ,  $\lambda_{max}$  and  $\sigma_1$  for all the 51 stars with their respective errors. The colour excess  $E_{B-V}$  for different observed stars are taken from the work of Joshi & Sagar (1983). Of the 51 stars observed, 14 of them have the unit weight error of the fit above the limiting value of 1.6 (member stars 174, 156, 143, 149, 138, 129, 123, 188, 136, 118 and non-member stars 363, 362, 130, 184). As mentioned above, the higher value of  $\sigma_1$  gives a clue about the presence of intrinsic polarization in the light from the star. So, in principle, in case of IC 1805, interstellar dust alone does not appear to be responsible for the observed polarization. There is also a indication of intrinsic polarization in measurements for some of the observed stars.

The observed normalized polarization-wavelength dependence of the stars in IC 1805 is shown in Figure 3. The solid curve denotes the Serkowski polarization relation for the general interstellar medium. In this plot, there exist a good agreement between theory and observations, which indicates that the observed polarization for the stars of IC 1805 is mainly due to Davis-Greenstein mechanism (Davis & Greenstein 1951) that operates in the general interstellar medium.

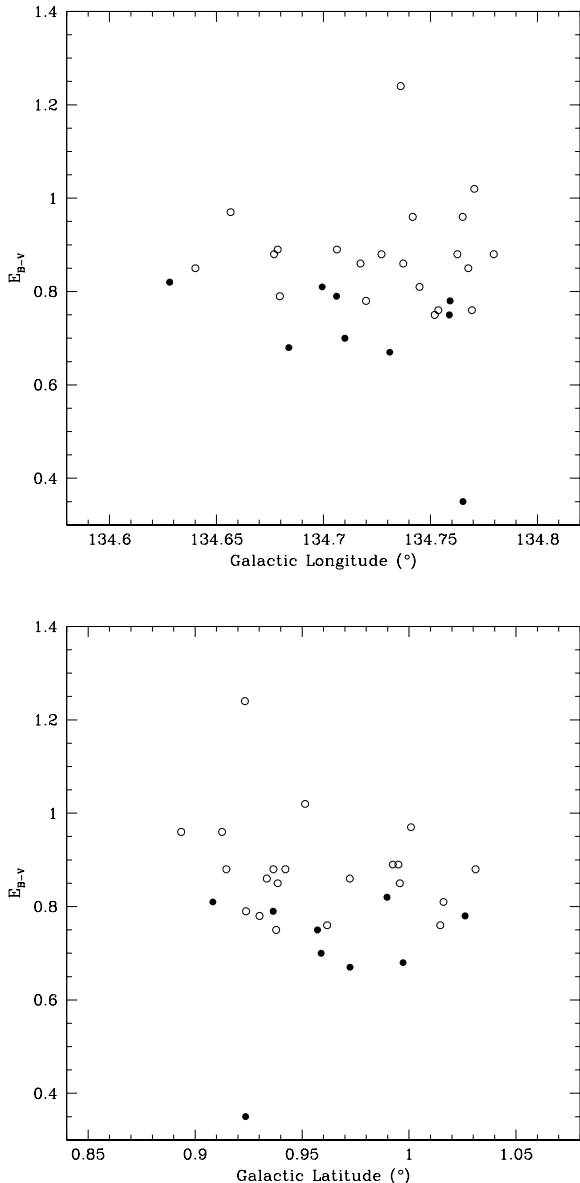


**Figure 5.** Top (5a): Colour excess  $E_{B-V}$  plotted as a function of galactic longitude ( $l$ ). Bottom (5b): Colour excess  $E_{B-V}$  plotted as a function of galactic latitude ( $b$ ). Excesses are taken from Joshi & Sagar (1983). Open circles indicate the observed member stars and filled circles indicate the *frontside* stars.

The foreground reddening toward IC 1805 is  $\sim 0.8$  mag and the reddening law is anomalous in this direction (Borgman 1961; Jhonson 1968; Ishida 1969; Turner 1976). In the direction of IC 1805 the interstellar reddening increases quite linearly up to 1 kpc with an average absorption of about 0.6 mag/kpc. This indicates that the distribution of interstellar material in the local arm is rather uniform. To remove the effect of interstellar dust located in front of IC 1805 or to determine the effect of *intracluster* dust on the members of IC 1805, we follow the method described by Marraco *et al.* (1993). In order to do the same, we have selected a group of 9 stars among the members of IC 1805, covering the whole observed region and which seems to be

**Table 4.** BVR polarization results

Id	$P_{max}$	$P_{max}$	$P_{max}$	$E_{B-V}$	$E_{B-V}$	$E_{B-V}$
	o	f	i	o	f	i
118	5.92	4.82	1.10	0.85	0.72	0.13
121	6.38	4.38	2.00	0.88	0.72	0.16
122	5.20	4.77	0.43	—	0.72	—
123	3.32	1.78	1.54	0.79	0.72	0.07
128	3.85	2.84	1.01	0.97	0.72	0.25
136	5.58	4.86	0.72	0.89	0.72	0.17
143	5.09	4.60	0.49	0.86	0.72	0.14
147	4.82	4.46	0.36	0.78	0.72	0.06
154	4.29	3.39	0.90	0.96	0.72	0.24
156	4.29	3.71	0.58	0.88	0.72	0.16
157	5.65	4.86	0.79	0.89	0.73	0.16
158	4.38	3.29	1.09	1.24	0.72	0.52
160	5.73	4.75	0.98	1.02	0.73	0.29
165	5.53	4.84	0.69	0.86	0.73	0.13
166	4.90	4.76	0.14	0.75	0.73	0.02
168	5.57	4.69	0.88	0.96	0.72	0.24
171	5.37	4.41	0.97	0.76	0.73	0.03
175	4.92	4.08	0.84	0.85	0.73	0.12
182	5.85	4.72	1.13	0.81	0.73	0.08
183	5.03	4.72	0.31	0.88	0.73	0.15
191	4.24	2.31	1.93	0.88	0.73	0.15
192	3.51	1.98	1.53	0.76	0.73	0.03

$P_{max}$  in % and  $E_{B-V}$  in mag.

o : observed

f : foreground

i : *intracluster*

least affected by the reddening. These stars hereafter referred to as *frontside* stars, they are indicated by  $^\dagger$  in Table 3. The *frontside* stars will be used to model the contribution of foreground excess, polarization and finally which will be removed from the remaining member stars to determine the *intracluster* parameters respectively.

Figure 4 shows the Galactic distribution ( $l, b$ ) of all the observed stars in the IC 1805. We have used open circles for all the observed stars and filled circles for the selected *frontside* stars. Figures 5a and 5b show the colour excess  $E_{B-V}$  plotted as a function of galactic longitude ( $l$ ) and latitude ( $b$ ) respectively, filled circles for the selected *frontside* stars and open circles for the other members.

In order to model the effect of foreground extinction, we fit the colour excesses  $E_{B-V}$  for the all nine *frontside* stars to a plane ( $l, b$ ). The final equation of the fit is

$$E_{(B-V)}(l, b) = 0.0886975l + 0.0905122b - 11.2302(mag.) \quad (6)$$

with an rms error of the unit weight of 0.05. The variation of the excesses with galactic longitude ( $l$ ) is the most significant part of the Marraco's model (Marraco *et al.* 1993). The observed, modeled and *intracluster* values of the colour excesses for the *non-frontside* stars are listed in Table 4. It can be mentioned that the modeled value of the *frontside* excess led to very small values of the *intracluster* excess.

The weighted mean of  $\lambda_{max}$  for nine *frontside* stars is

$$\overline{\lambda_{max}} = 0.544 \pm 0.005 \text{ } (\mu\text{m}) \quad (7)$$

This value is quite similar to Guetter *et al.* (1989) for the cluster IC 1805 ( $0.54 \pm 0.01 \text{ } \mu\text{m}$ ). Moreover, this value does not differ more from the *intracluster* value of  $\lambda_{max}$

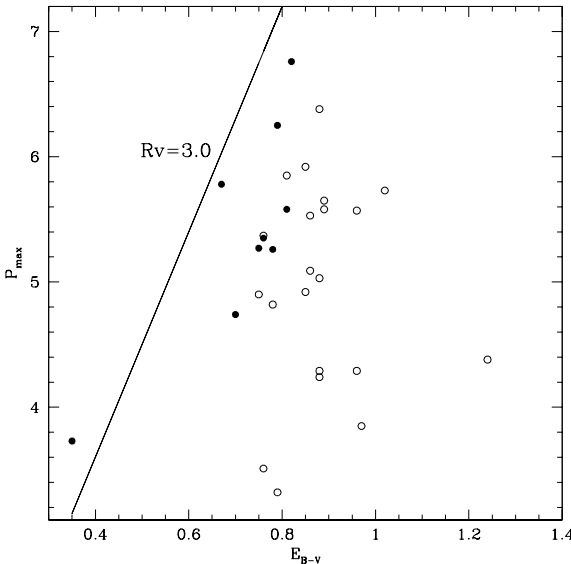


**Figure 6.** Polarization efficiency diagram for the observed dust. Using  $Rv=3.0$ , the line of maximum efficiency drawn. Filled and open circles indicate *frontside* and *non-frontside* members of IC 1805.

$(0.541 \pm 0.003 \mu\text{m})$ . These values are very close to the mean interstellar value of  $\lambda_{max} 0.56 \pm 0.04 \mu\text{m}$  (Serkowski *et al.* 1975). Therefore, we can conclude that the characteristic particle size distribution as indicated by the polarization study of stars in IC 1805 is essentially the same as that for the general interstellar medium.

In case of polarization, the weighted mean of maximum polarization  $P_{max}$  for nine *frontside* stars is

$$\overline{P_{max}} = 4.865 \pm 0.022 \text{ \%} \quad (8)$$

and the weighted mean of maximum polarization  $P_{max}$  for the cluster member is  $5.008 \pm 0.005 \text{ \%}$ . So, there is also no vast difference between *frontside* and *intraccluster* polarization, the contribution of the *intraccluster* material on polarization is  $\simeq 3 \text{ \%}$ . The weighted mean of the polarization position angle  $\theta_V$  for nine *frontside* is  $120.00 \pm 0.06$ . It is possible to calculate  $\bar{u}$  and  $\bar{q}$ , the mean value of normalized Stokes parameters for the group of nine *frontside* stars. Subtracting this mean value from individual  $u$  and  $q$  for the rest of the observed members of IC 1805 and inverting the procedure, we obtained the values of  $P_{max}$  for *intraccluster* medium and list them in Table 4.

In diffuse interstellar medium the polarization efficiency (ratio of the maximum amount of polarization to visual extinction) can not exceed the empirical upper limit,

$$P_{max} < 3A_V \simeq 3R_V \times E_{B-V} \quad (9)$$

which is obtained for interstellar dust particles (Hiltner 1956). The ratio  $P_{max}/E_{B-V}$  mainly depends on the alignment efficiency, magnetic strength and also the amount of depolarization due to radiation traversing more than one cloud with different direction. Figure 6 shows the relation between  $P_{max}$  and colour excess  $E_{B-V}$  for the members and *frontside* stars of IC 1805. Except the *frontside* star 170, no star lie at the left block of the interstellar maximum

line. Though, the *frontside* star-170 falls at the left block of the interstellar maximum line, but the value of  $\sigma_1$  for the star-170 is 0.63 (unit weight error of fitting of Serkowski polarization relation [Eq.(5)]), which is much below than the limiting value 1.6. So, there is very less possibility of having intrinsic polarization in star-170. The polarization efficiency plot for the members of IC 1805 indicates that apparently the stars are not affected by intrinsic polarization. The dominant mechanism of polarization in the observed section of IC 1805 is supposed to be the alignment of grains by magnetic field, in a similar way as that found in the general interstellar medium.

## 5 CONCLUSIONS

The main results of the *BVR* polarimetric study of IC 1805 can be summarized as follows:

The mean value of maximum polarization  $P_{max}$  of IC 1805, for foreground is  $4.865 \pm 0.022 \text{ \%}$  and while for the *intraccluster* medium is  $5.008 \pm 0.005 \text{ \%}$ . The contribution of the *intraccluster* dust on polarization is  $\simeq 3 \text{ \%}$ .

The mean wavelength dependence of polarization  $\lambda_{max}$  for the cluster member is  $0.541 \pm 0.003 \mu\text{m}$  and for foreground is  $0.544 \pm 0.005 \mu\text{m}$ . The very less dispersion of  $\lambda_{max}$  indicates that the mean *intraccluster* grain size is quite similar to general interstellar medium.

Though the observed polarization of some of the stars in IC 1805 may be due to intrinsic stellar polarization in their measurements, but the dominant mechanism is polarization due to the general interstellar medium. The difference between foreground and *intraccluster* colour excess is negligible in the direction of IC 1805. There is very little evidence of dust in the *intraccluster* region. The highly polarized and reddened stars may be projected through various discrete foreground clouds, which have different grain sizes and compositions.

## ACKNOWLEDGMENTS

This research has made use of the WEBDA database, operated at the Institute for Astronomy of the University of Vienna, use of image from the National Science Foundation and Digital Sky Survey (DSS), which was produced at the Space Telescope Science Institute under the US Government grant NAG W-2166, use of NASA's Astrophysics Data System and use of IRAF, distributed by National Optical Astronomy Observatories, USA. We thank the referee for his constructive comments which have lead to a considerable improvement in the paper. The author (BJM) would like to thanks Orchid, Amitava, Manash, Sanjeev and Jessy for their support.

## REFERENCES

- Borgman, J., 1961, Bull. Astron. Inst. Neth., 16, 99
- Clayton, Geoffrey C., Cardelli, Jason A., 1988, AJ, 96, 695
- Coyne, G. V., Magalhaes, A. M., 1979, AJ, 84, 1200
- Davis, L. Jr., Greenstein, Jesse L., 1951, ApJ, 114, 206
- Guetter, Harry H., Vrba, Frederick J., 1989, AJ, 98, 611
- Hiltner, W. A., 1956, ApJS, 2, 389

Ishida, K., 1969, MNRAS, 144, 55  
Johnson, H. L., 1968, Nim.book, 167  
Joshi, U. C., Sagar, Ram, 1983, JRASC, 77, 40  
Kwon, Suk Minn, Lee, See-Woo, 1983, JKAS, 16, 7  
Marraco, H. G., Vega, E. I., Vrba, F. J., 1993, AJ, 105, 258  
Massey, P., Johnson, K. E., Degioia-Eastwood, K., 1995, ApJ, 454, 151  
McMillan, R. S., 1978, APJ, 225, 880  
Ramaprakash, A. N., Gupta, R., Sen, A. K., Tandon, S. N., 1998, A&AS, 128, 369  
Rautela, B. S., Joshi, G. C., Pandey, J. C., 2004, BASI, 32, 159  
Sagar, Ram, 1987, MNRAS, 228, 483  
Sagar, Ram, Yu, Qian Zhong, 1990, ApJ, 353, 174  
Sanders, W. L., 1972, A&A, 16, 58  
Sanders, W. L., 1971, A&A, 14, 226  
Schmidt, G. D., Elston, R., Lupie, O. L., 1992, AJ, 104, 1563  
Serkowski, K., 1973, IAUS, 52, 145  
Serkowski, K., Mathewson, D. L., Ford, V. L., 1975, ApJ, 196, 261  
Shi, H. M., Hu, J. Y., 1999, A&AS, 136, 313  
Tinbergen, J., 1996, Introduction to Astronomical Polarimetry, Cambridge University Press.  
Turner, D. G., 1976, AJ, 81, 1125  
Vasilevskis, S., Sanders, W. L., van Altena, W. F., 1965, AJ, 70, 806  
Wilking, B. A., Lebofsky, M. J., Kemp, J. C., Martin, P. G., Rieke, G. H., 1980, ApJ, 235, 905  
Whittet, D.C.B., van Breda, I.G., 1978, A&A, 66, 57

This paper has been typeset from a  $\text{\TeX}$ /  $\text{\LaTeX}$  file prepared by the author.